Screen printed $La_{2/3}Sr_{1/3}MnO_3$ thick films on alumina substrates

L. Durand, Ll. Balcells, A. Calleja, J. Fontcuberta, and X. Obradors
Institut de Ciència de Materials de Barcelona (CSIC), Campus Universitat Autònoma de Barcelona,
E-08193 Bellaterra, Catalunya, Spain

We report here on the preparation of $La_{2/3}Sr_{1/3}MnO_3$ magnetoresistive thick films on polycrystalline Al_2O_3 substates by using the screen printing technique. It is shown that films can be obtained using high temperature sintering. While there is a reacted layer, this improves adhesion and is not too troublesome if the films are made thick enough. It is shown that $PbO-B_2O_3-SiO_2$ glass additives allow sintering at lower temperatures and can be used to improve the mechanical stress of the films. However, it is found that glass concentrations large enough to significantly improve the film adherence result in a weak low field magnetoresistance probably because grains are coated with high resistivity material. Strategies to overcome these difficulties are discussed.

I. INTRODUCTION

Magnetoresistive materials based on manganese perovskites of $L_{1-x}A_xMnO_3$ type, where L is a lanthanide and A is a divalent alkaline-earth are currently being intensively studied.[1] Aside from its scientific interest related to their rich physical properties, the expectation of useful materials for technological applications promotes research on materials of enhanced field sensitivity and in a form suitable for device fabrication.

The discovery that grain boundaries and interfaces[2–4] can be important sources of low-field magnetoresistance (LFMR) has stimulated renewed interest on ceramic or granular $L_{2/3}A_{1/3}MnO_3$ oxides. Tailoring of artificial interfaces by using appropriate substrates and epitaxial thin film technologies is being initiated.[5] In brief, it appears that magnetic scattering or tunneling of polarized charge carriers across interfaces is extremely sensitive to applied magnetic fields. Therefore, the current issue is to understand and modify the nature of interfaces and the magnetic coupling across them. Two different strategies have so far been reported: the modification of the magnetic surface frustration of grains by appropriate tailoring of the intragrain magnetic interaction strength[4] and the change of the magnetic coupling through interfaces by changing the grain boundary angles.[5]

However, even if the LFMR could be optimized, to get a chance for technological applications, $L_{2/3}A_{1/3}MnO_3$ materials still face the problem of development of a suitable low cost technique for film fabrication. The screen printing technique appears to be appropriate; it can be scaled up easily, and it is widely used in fabrication of solid state devices and sensors in industrial environments. Rather preliminary results concerning the use of the screen printing technique to grow thick films of $L_{2/3}A_{1/3}MnO_3$ have been recently reported.[6]

The aim of this paper is twofold. First, we would like to explore the conditions for optimal growth of $L_{2/3}A_{1/3}MnO_3$ (LSMO) thick films on low-cost substrates. Polycrystalline Al_2O_3 substates will be used. In order to improve the mechanical strength of the films, it will become necessary to investigate the use of additives. A $PbO-B_2O_3-SiO_2$ glass has been chosen because of its low melting point. Grain coating with a thin insulating layer may, in principle, modify the grain surfaces and thus the magnetotransport properties. This is the second objective of this paper.

II. EXPERIMENTAL

A. The $La_{2/3}Sr_{1/3}MnO_3$ powder synthesis

Ceramics of $La_{2/3}Sr_{1/3}MnO_3$ (LSMO) composition were prepared by the standard solid state reaction method. Dried La_2O_3, $SrCO_3$, and MnO_2 were used as starting materials, weighted in the appropriate ratios, and mixed and homogenized in an agate ball-milling device (30 min). After pelletizing, the solid state reaction was performed, under air atmosphere. Synthesis involved at least four thermal steps: 15 h at 900 °C, 15 h at 940 °C (repeated twice), and a final step at 1400 °C for 4 h. Samples were ground and pelletized at each step.

In the following it will be necessary to study properties of films prepared by using LSMO ceramics of different grain size. To this purpose, after the last reaction step, the pellets have been powdered by using two different techniques. In the first, the pellets were crushed in an agate ball mill for 2 h. The resulting powder from this batch (A) was further refined by using an attritor, to produce batch B. In the attritor, powder A was mixed with acetone and zirconia balls and shaken for three days. X-ray diffraction of powders A and B do not

2623

show any traces of secondary or impurity phases. The x-ray patterns of both samples were identical, except for the noticeable broadening of the reflections of sample B (Fig. 1), which was in fact used to estimate the mean size of the coherent diffracting volume (minimal particle size). In agreement with images obtained by scanning electron microscopy (SEM), the grain size of sample B is in the 0.1 μm range, much smaller than that of batch A ($\Phi \approx 1$–4 μm). The SEM pictures for both samples, shown in Fig. 2, clearly reveal the reduced size of powders from batch B.

B. Synthesis of the composite glass/ La$_{2/3}$Sr$_{1/3}$MnO$_3$

To fulfill the requirements of a low melting temperature and convenient reactivity with the substate, the composition of the glass should be appropriately chosen. A glass of 63 wt. % PbO – 25 wt. % B$_2$O$_3$ – 12 wt. % SiO$_2$ was prepared by mixing the appropriate amounts of the corresponding oxides and, after mixing in the ball mill, heating up to 900 °C. It is known that this mixture melts at about 820 °C and reacts with alumina (Al$_2$O$_3$).[7] The melted mass is kept at this temperature for 15 min before quenching to room temperature. The obtained glass is ground down to large grains (3–30 μm) (Glass GL1) or to smaller grains (1–10 μm) (Glass GL2) by using the ball mill (0.5 h or 16 h, respectively).

The resulting powders have been subsequently carefully mixed (1 h ball milled) with the ceramic LSMO powders (batch A). Different mixing ratios of glass/ceramics have been explored, ranging from 2 wt. % to 10 wt. %.

C. Screen printing

The screen printing technique is described elsewhere.[8] Basically, an ink is prepared by using the ceramic powder and an organic vehicle and spread through a screen of the appropriate aperture on a substrate. In the present case, the substrates are polycrystalline (5 mm $\times$ 5 mm) Al$_2$O$_3$ (Meller Optic, Inc.) polished down to 1 μm. Preparation of films by the screen printing technique involves three key steps that strongly determine the final characteristics of the films: (a) the preparation of the ink, (b) the selection of the screen open area, and (c) the thermal treatment. In the following we shall describe these steps.

(a) The reologic properties of the ink determine the film morphology. We have chosen the RV025 organic vehicle from Heraeus.[5] It decomposes at about 450 °C, in air, without solid residues. To prepare the mixture LSMO/RV025, the specific surface of the powder and the wetting properties of the organic vehicle are limiting factors.
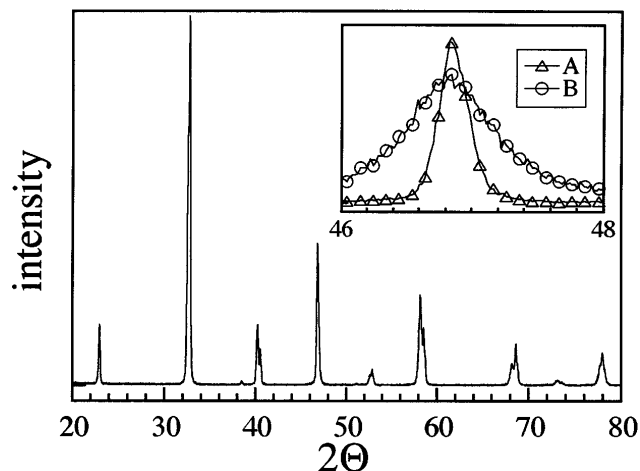

FIG. 1. X-ray diffraction patterns of La$_{2/3}$Sr$_{1/3}$MnO$_3$ samples from batches A and B. Main: sample from batch B. Inset: Comparison of a reflection for A and B samples.

After several trials, it turns out that the optimal ratio for powders from batch A ($\Phi \approx 1$–4 μm) is 2 : 1 (wt.). This mixture is gently shaken in the agate mortar for 1 h. It is extremely important to mention that after this process the ink is stable (no sedimentation) for long periods of time (at least 24 h), thus allowing repeated printing experiments without appreciable modification of the reology of the ink.

We failed to prepare homogeneous inks using the powders of batch B which have smaller particle size ($\Phi \approx 0.1$ μm). It turns out that the inks prepared using these powders are not fluid enough even at lower powder/RV025 ratios. In addition, homogenization in the ball mill did not succeed and the resulting ink was still clustered. These effects, probably related to the enhanced specific surface of particles of batch B and their magnetic interaction, could not be overcome and other dispersants should be investigated. Consequently, in the following only results obtained using inks made from powders of batch A will be presented.

(b) Selection of the screen open area (OA). Commercial screens are available having a variety of open areas. The OA is defined by the ratio of the screen aperture and the string thickness, and it determines the thickness and flatness of the printed film. Of course, using a particular aperture requires a convenient (smaller) particle size of the ceramic charge of the ink. We have explored several OA. Here we present the results obtained by using the so-called SCR1 (OA = 32) and SCR2 (OA = 43) screens which will lead to films of thickness of about $t \approx 10$ μm and $t \approx 20$ μm, respectively.

Printing of the substrate is manually done by spreading the ink on the screen, which is placed on top of the substrate.
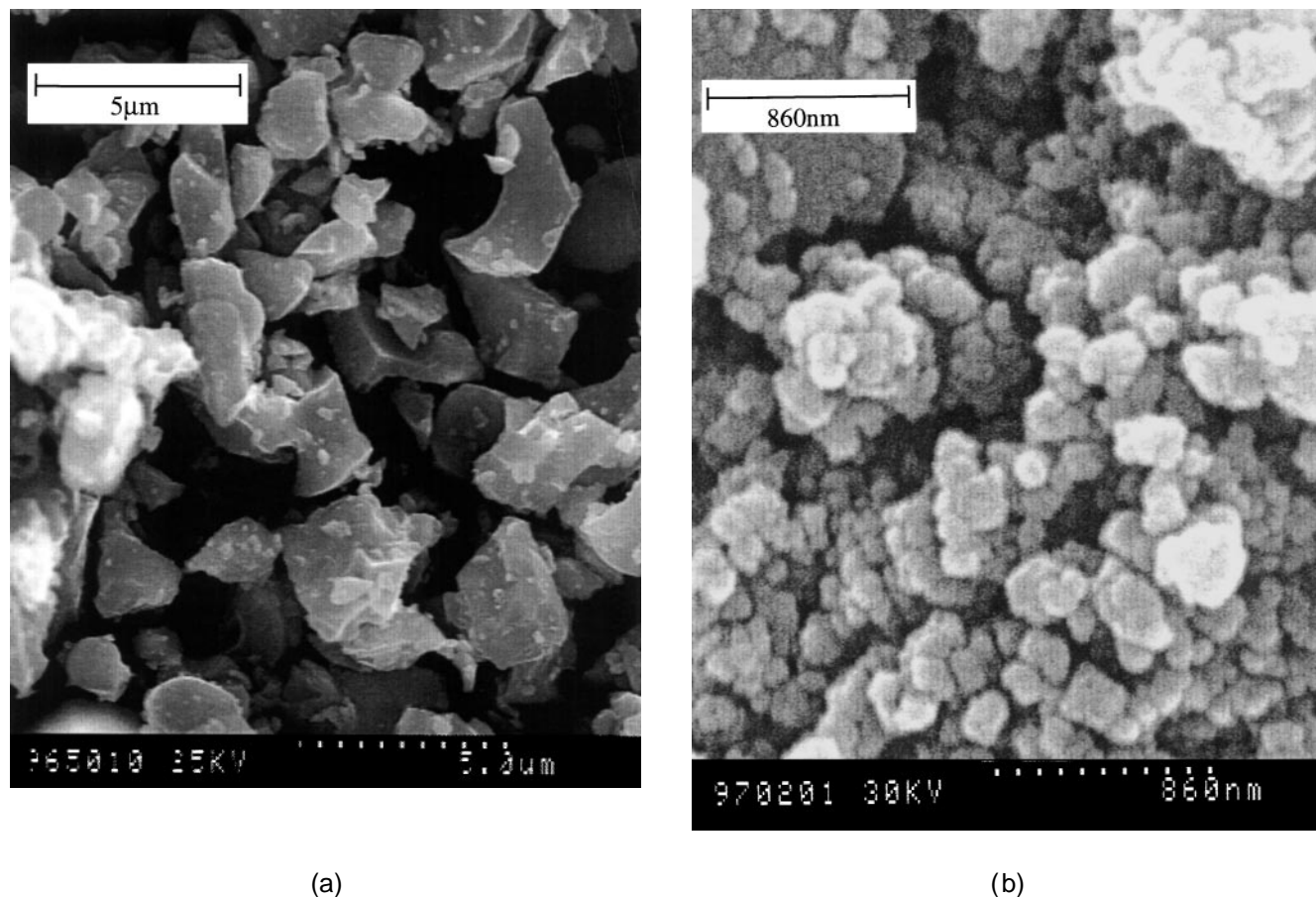
(a)

(b)

FIG. 2. SEM for powders of batches (a) A and (b) B, respectively. Notice the different scale for both pictures.

(c) The thermal treatment involves two stages. In the first one (at about 450 °C), the thermal decomposition of the organic vehicle takes place. In the second, at a temperature T_m, sintering of the film occurs. Heating and cooling has always been performed at fixed conditions (±300 °/h). All these processes are performed under an oxygen flow to ensure complete combustion of the organic carrier.

For films prepared using pure LSMO, the final temperature T_m has been varied from 900 °C to 1400 °C in order to explore the optimal sintering conditions. For films prepared using glass/LSMO mixtures, the sintering temperature has been fixed at $T_m = 840$ °C, about 20 °C above the melting point of the glass. The films have been kept at $T = T_m$ for 0.1 h in the first case and 0.2 h in the second case.

D. Microstructural and physical characterization

Electrical resistivity has been measured by using the four-probes configuration in the 10–375 K temperature range under fields up to 50 kOe by using a superconducting coil. Electrical contacts have been made by using silver paste or silver epoxy. Magnetization

measurements have been simultaneously performed by using a Quantum Design SQUID magnetometer.

A Hitachi S-570 scanning electron microscope has been used for microstructural analysis. Film/substrate interfaces were studied on polished cross sections by using an energy dispersions x-ray analysis (EDX) system coupled to a JEOL JSM-6300 electron microscope.

III. RESULTS AND DISCUSSION

Presentation of experimental results and discussion will be performed separately for films prepared by using pure LSMO and films prepared by using Glass/LSMO mixtures.

A. La$_{2/3}$Sr$_{1/3}$MnO$_3$ screen printed films

Films prepared by using SCR1 have a thickness of about $t \approx 10$ μm. As shown in Fig. 3 the grain size and connectivity improve markedly when increasing T_m. At the highest T_m, grains larger than 2 μm are commonly found, well connected, and with a characteristic terrace-like shape. This can be better appreciated in Fig. 3(b) where an enlarged view of the intergranular zone for $T_m = 1400$ °C is shown. The adherence of the film to the alumina substrate is only good for $T_m = 1400$ °C,
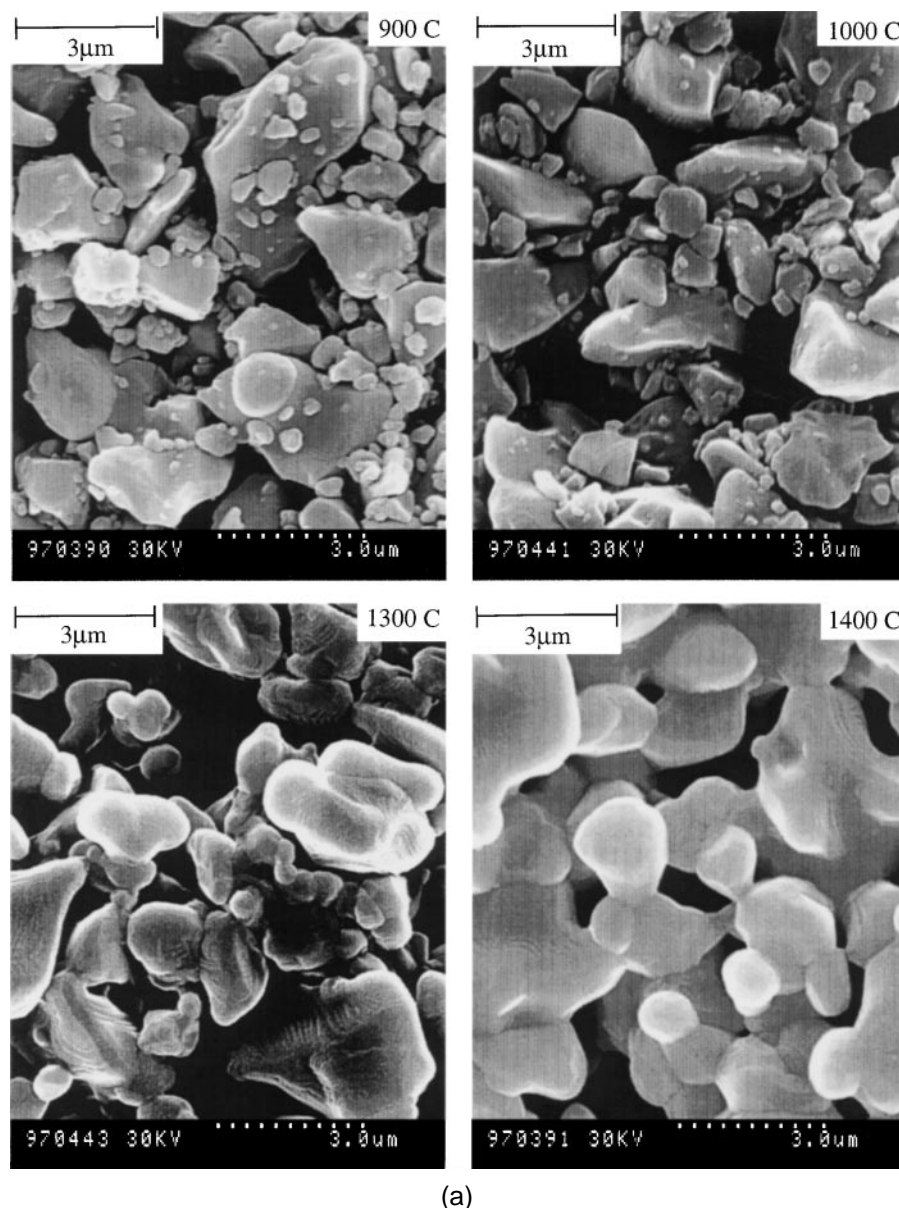
FIG. 3. (a) SEM view of the SCR1 films surfaces prepared at various firing temperatures: T_m = 900 °C, 1000 °C, 1300 °C, and 1400 °C. (b) Expanded SEM view of the SCR1 film at T_m = 1400 °C (scale 1 μm).

and it deteriorates rapidly when decreasing the sintering temperature. Good substrate-film adherence suggests the presence of some reacted layer at the interface. Films prepared by SCR2, having a thickness of about $t \approx$ 20 μm, display similar features. To explore the interface, SEM cross section observations have been performed on a T_m = 1400 °C, SRC2 film. In Fig. 4 we show the back scattering electron (BSE) and EDX images of this film. Inspection of these images several important aspects. First, a strong interface reaction is observed in the BSE image: an interdiffusion layer of about 4 μm within the alumina can be clearly appreciated. The accompanying EDX pictures indicate that Sr, La, and Mn all diffuse

from the film toward the substrate. Significantly, at the interface, Sr is almost depleted in a layer of about 3 μm.

This strong chemical reaction between the LSMO film and the substrate provides the required adherence, but it should change the physical properties of the film itself. Notice that in a film of $t \approx$ 20 μm (SCR2) the interdiffusion layer is about 15% of the total thickness.

Similar experiments performed on films sintered at T_m = 1200 °C do not show significant traces of reactivity. However, for these samples, as mentioned above, adherence was not good enough.

In order to explore the effects of sintering and interdiffusion, extensive magnetotransport measurements
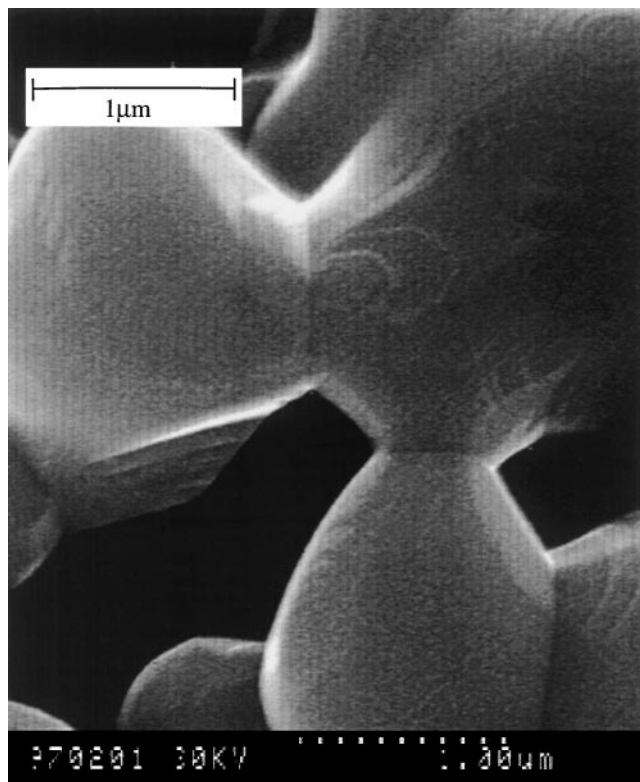
(b)

FIG. 3. (*continued from previous page*)

have been performed. In Fig. 5(a) we present the temperature dependence of the resistivity $\rho(T)$ for all SCR1 films. The most prominent feature of Fig. 5(a) is that when increasing T_m the resistivity significantly decreases owing to the improved grain connectivity as shown in the SEM pictures of Fig. 3. More subtle is the shift in

temperature of the maximum of $\rho(T)$. We recall that the maximum of $\rho(T)$, occurring at T_M, is reminiscent of the Curie temperature and in single crystals, epitaxial films, and well-connected ceramics indicates the onset of ferromagnetic ordering in the sample. In the present case, when increasing T_m (900–1300 °C), T_M shifts first toward higher temperatures, but at 1400 °C lowers again. This behavior can be better appreciated in Fig. 5(b) where the temperature dependence of the normalized resistivity is displayed.

On the basis of the data shown by the SEM pictures of Figs. 3–4, the electrical properties of the films can be simply understood: the lowering of the resistivity and the initial rise of T_M where $\rho(T)$ is maximum reflects the improved grain connectivity, whereas the subsequent lowering of T_M for higher sintering temperatures (1400 °C) should result from the ionic interdiffusion with the substrate. In fact, it is well known, for instance, that Al intercalation in LSMO results in severe degradation of the Curie temperature.[9] In order to corroborate this hypothesis, we have measured a set of ceramic samples, prepared by using the very small sized initial LSMO powders of batch B, and sintered at different temperatures (700–1400 °C). The results, shown in Fig. 6, display the expected trend when increasing T_m, T_M shifts toward higher temperatures. Notice that, in the absence of film-substrate interaction the film sintered at 1400 °C has the maximum of $\rho(T)$ at about 360 K as observed in single crystals.[10]

It is clear that reactivity of the film with the substrate would have minor importance when the film thickness increases. In fact, that was the reason to prepare films by using SCR2. As shown by the $\rho(T)$ data of Fig. 5, for the SCR2 films the resistivity maximum is already observed at a temperature coincident with that observed for ceramics, thus proving that interdiffusions has a neg-
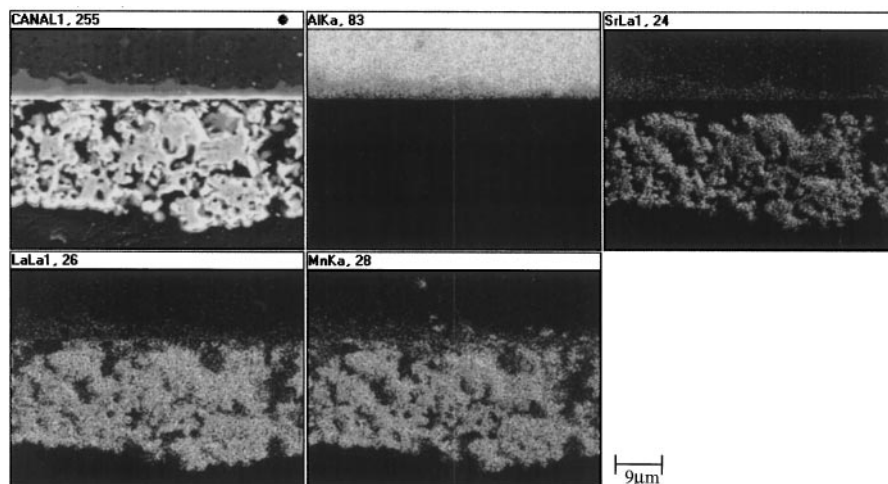
FIG. 4. Backscattering electron (BSE) and EDX cross section images of the $T_m = 1400$ °C film.
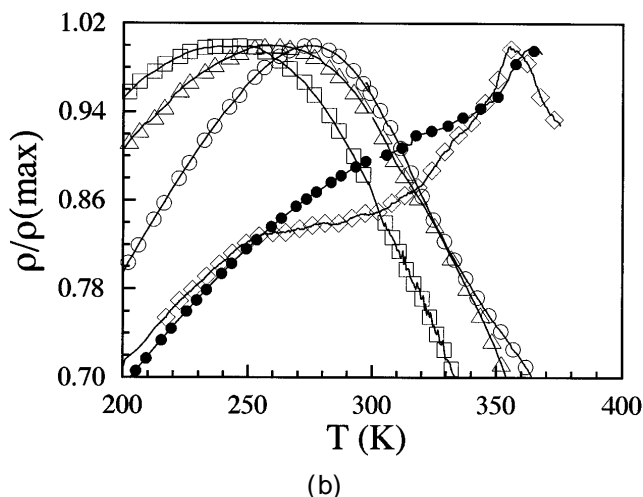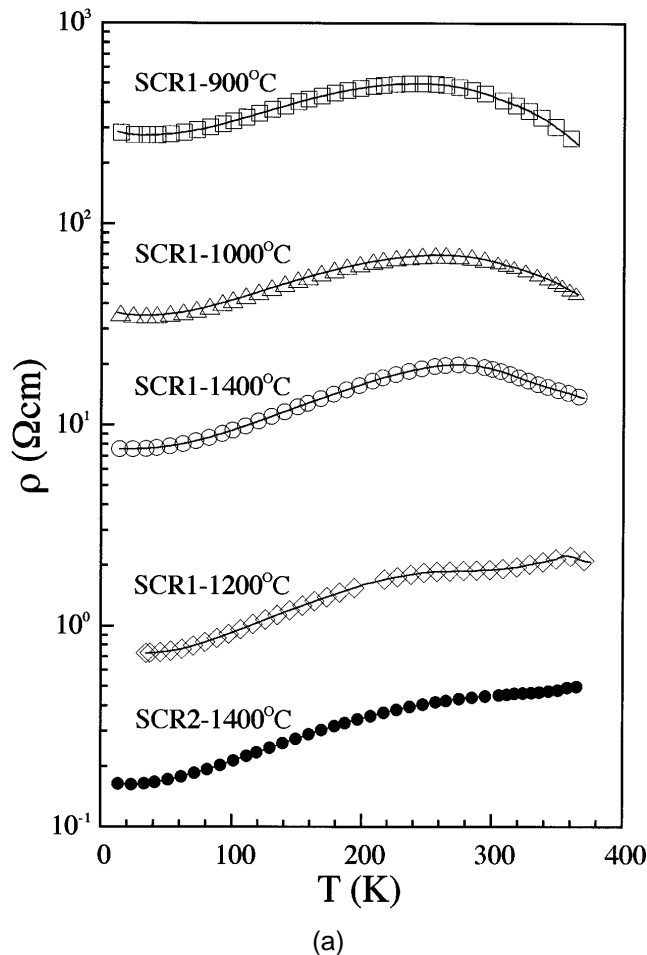
(a)

(b)

FIG. 5. (a) Temperature dependence of the resistivity $\rho(T)$ for SCR1 films: T_m = 900 °C, 1000 °C, 1200 °C, and 1400 °C and SCR2 at 1400 °C. (b) Temperature dependence of the normalized resistivity $\rho(T)/\rho(T_m)$ for SCR1 and SCR2 films. Symbols are as in (a).

FIG. 6. Temperature dependence of the resistivity $\rho(T)$ for La$_{2/3}$-Sr$_{1/3}$MnO$_3$ ceramics: T_m = 700 °C, 900 °C, 1100 °C, and 1400 °C.

is the zero field resistivity, of about 1% at 1 kOe is observed.

B. Glass/La$_{2/3}$Sr$_{1/3}$MnO$_3$ screen printed films

A preliminary task is to evaluate the role of the initial particle size of the glass on the film homogeneity after sintering and melting at a fixed temperature (840 °C). To that purpose films have been printed, using SCR1 and LSMO powders of batch A ($\Phi \approx 1-4 \ \mu$m), and glasses GL1 (3–30 μm) and GL2 (1–10 μm) in a glass/ceramics ratio of 10 wt. %. The SEM images reveal that films prepared with the smaller glass particle size (GL2) are homogeneous and with a smooth surface, whereas those films prepared using the larger particles GL1 are rather inhomogeneous, with some remarkable holes on the surface (Fig. 8). It is believed that these holes are formed during the melting of the glass at about 820 °C. Naturally, this effect becomes more prominent when increasing the size of the glass particles.

The next task is to explore the distribution of glass within the ceramic matrix. The EDX images obtained

ligible effect. The field dependence of the magnetization and resistivity of this SCR2, 1400 °C film is shown in Fig. 7. A magnetoresistance MR = $\rho(H)/\rho_0$, where ρ_0
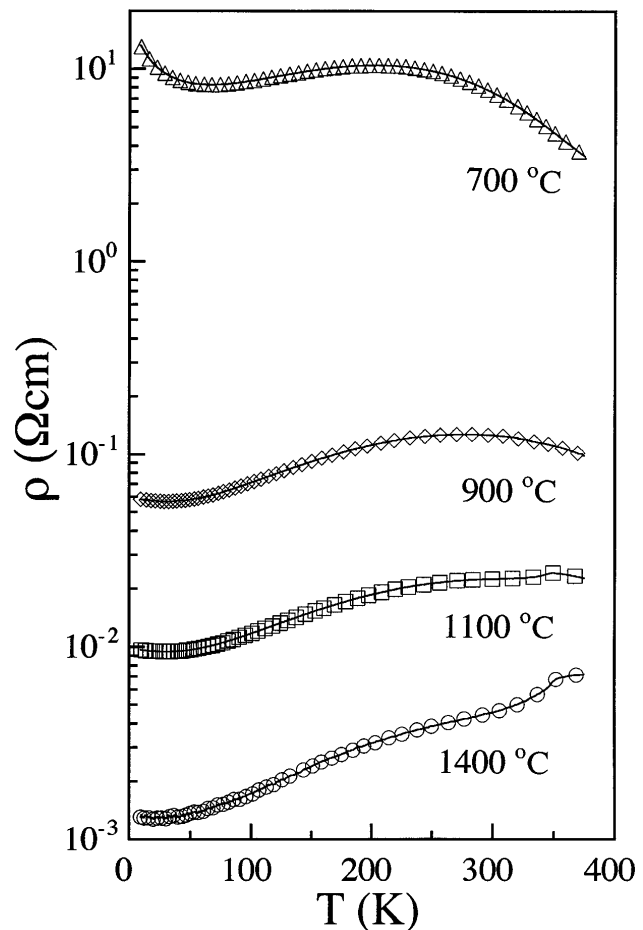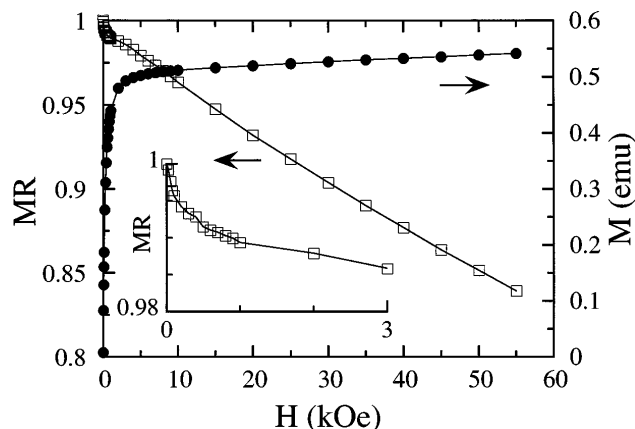
FIG. 7. The field dependence of the magnetization M (solid symbols) and resistivity $\rho(H)/\rho(H=0)$ (open symbols) for the SCR2, 1400 °C film at 300 K. Inset: The low-field region of $\rho(H)/\rho(H=0)$ is shown. Axes are as in main figure.

reveal the absence of aggregates of glass (Pb rich granules), but instead they indicate an homogeneous Pb distribution, thus suggesting that a glass film has coated the ceramic grains. On the other hand, as mentioned above, glass is expected to progress through the grains toward the substrate and to react partially with alumina, thus enhancing adherence of the film to the substrate. In fact, EDX cross-section mapping performed on a 5%-glass film (Fig. 9) reveals that some Al interdiffusion toward the LSMO film has occurred. Notice in upper-central image in Fig. 9 that some *gray spots* (corresponding to Al) are visible well within the film. Films prepared using GL2 and different glass/LSMO ratios (2%, 3.5%, 5%, and 10%) display a similar microstructure. Film and grain adherence improve as the ink becomes glass rich; however, it should be mentioned that good adherence is reached only for 10% glass. Therefore, glass addition provides a convenient way to improve mechanical strength of the film. In the following we will explore the effects of glass addition on their magnetotransport properties.

The electrical resistivity of the glass/ceramic composite films increases when increasing the glass content. More relevant, however, is the shape of the $\rho(T)$ curves for films of different glass concentrations. It can be observed in Fig. 10 that the residual resistance increases when increasing the glass content, to the point that the characteristic maximum of $\rho(T)$ at T_M is almost washed out for the 5% and 10% films. It is also observed that for the 2–3.5% films, T_M occurs well below the Curie point (T_c) observed in well-connected ceramics and single crystals. The shift of T_M with respect to T_c is not related to a possible significant interdiffusion of Al or other ions into the LSMO lattice. In fact, the magnetization of all films are coincident and signal a T_c of about 360 K. In Fig. 11 we show the magnetization versus
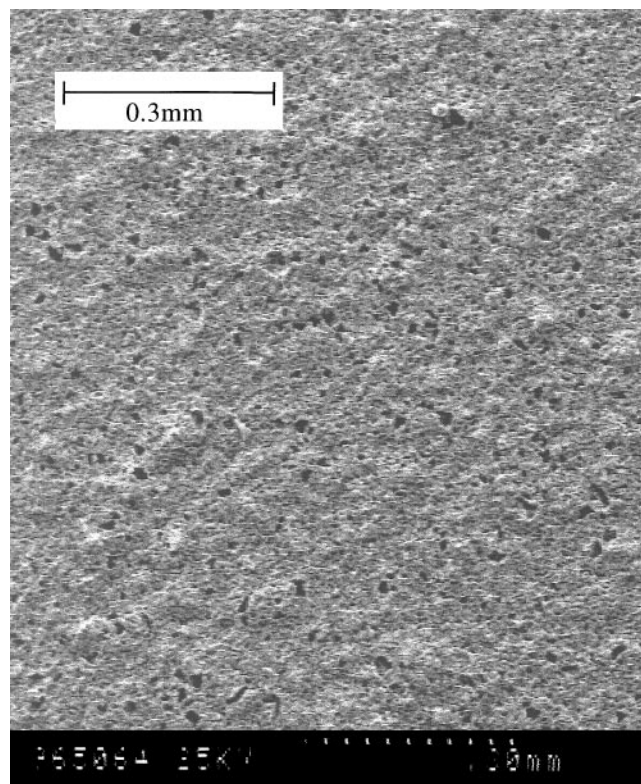
(a)
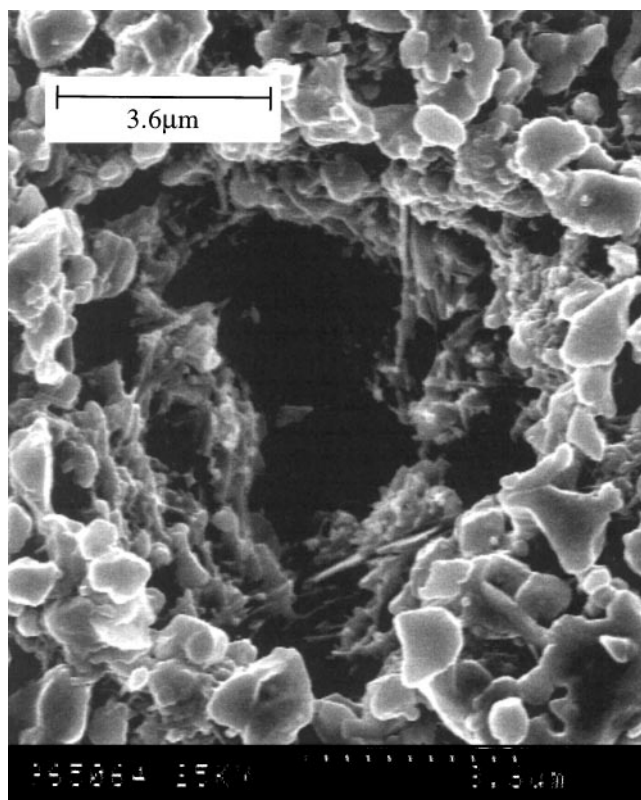
(b)

FIG. 8. The SEM images of film GL1 are shown. Notice the different scale in both figures: (a) scale = 0.3 mm; (b) scale = 8.6 μm.
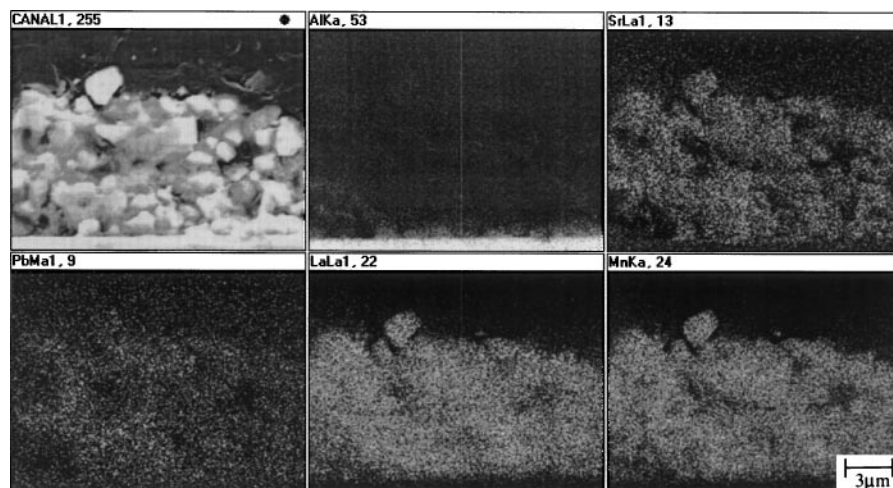
FIG. 9. Transverse EDX images obtained of GL2 films.

temperature measured at 10 kOe. The coincidence of these curves excludes any interdiffusion effect on the properties of the individual grains and strongly indicates that T_M is related to grain connectivity and to the presence of the intergranular glass coating. Therefore, the gradual lowering of T_M when increasing the glass content (Fig. 10) indicates that the glass coating degrades the intergranular magnetic coupling.

As mentioned above, the recent experimental results suggested[2–4] that scattering or spin diffusion at grain boundaries may have severe influence on the low field magnetoresistance. Therefore, having observed that grains are coated by glass, it is interesting to explore the magnetoresistance of these glass/ceramic films. Magnetoresistivity has been measured for these samples at several temperatures as a function of field. In

Fig. 12 we show MR $= \rho(H)/\rho_0$ where ρ_0 is the zero field resistivity for several samples at 5 K.

The overall shape of MR is similar to that reported for other ceramics. The initial low-field drop of resistance is apparent of the 2% and 3.5% films, but is almost washed out for the more resistive films (5% and 10%). Similarly, the total change of resistance at 50 kOe is much smaller for the films having higher glass concentration. A convenient way to extract the low-field magnetoresistance (LFMR) is to extrapolate the high field linear behavior toward zero field,[2] LFMR $= 1 - \lim_{(H\to 0)}$ (MR). In Fig. 12 (inset) we show the LFMR measured at several temperatures. It is clear that LFMR is vanishingly small for the 5% and 10% films but it is of about 20% for the less glass charged samples. At this point, it is worth comparing the LFMR of the
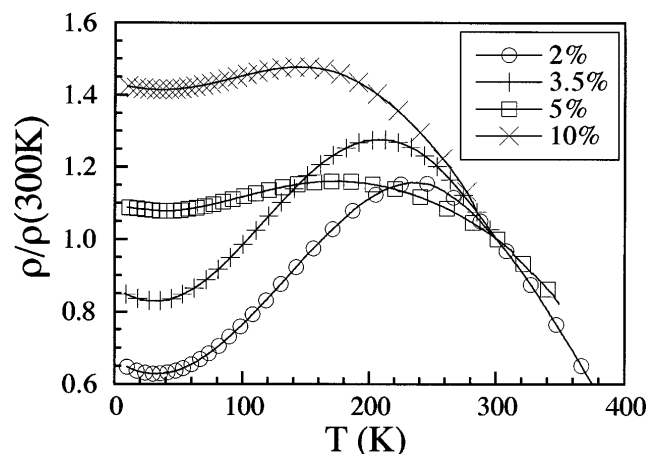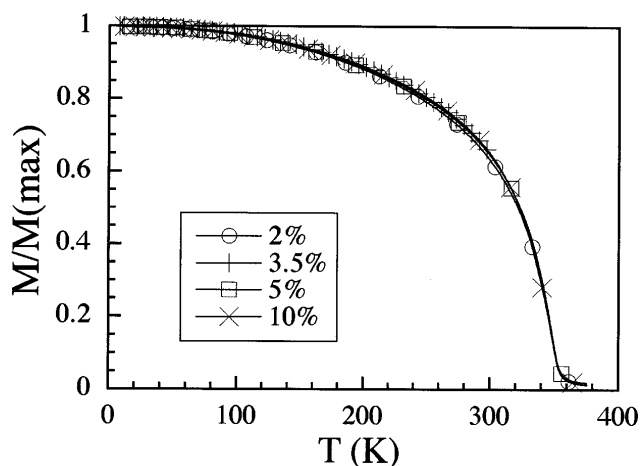

FIG. 10. Temperature dependence of the normalized resistivity $\rho(T)/\rho(300\,\mathrm{K})$ for glass/ceramic films: 10%, 5%, 3.5%, and 2%.

FIG. 11. Magnetization versus temperature measured at 1 kOe for the glass/ceramic films (10%, 5%, 3.5%, 2%). For clarity only a few of the experimental points are plotted. The solid lines represent the complete set of measure data.
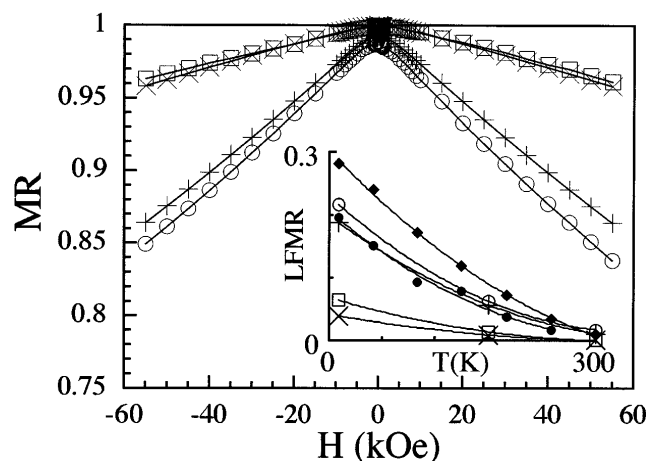
FIG. 12. Magnetoresistance MR $= \rho(H)/\rho_0$ where ρ_0 is the zero field resistivity for several samples at 300 K (symbols are as in Fig. 11). Inset: LFMR at several temperatures for the films: 10%, 5%, 3.5%, 2%, and for the ceramics sintered at 1400 °C (circles) and 700 °C (rhombus) (solid symbols).

glass/LSMO films with that measured for the ceramic samples Fig. 6. In Fig. 12 (inset) we have included for comparison the LFMR of the ceramics sintered at the extreme temperatures (700 °C and 1400 °C). It is clear that the introduction of a small amount of glass, allowing film growth at lower temperatures, results in LFMR values comparable to those measured for pure LSMO films prepared at 1400 °C. Of course, the mechanical characteristic of those films are somewhat better (especially for 10% glass) although the LFMR has been degraded by glass addition. We note that the LFMR reduction probably reflects the increasing importance of a nonmagnetoresistive contribution to the overall resistivity when increasing the glass content in the films. Therefore, any possible glass reinforced magnetic decoupling is overcome by the genuine rising of the resistivity of the sample. We thus should conclude that grain coating with highly resistive materials will not provide better LFMR ratios.

IV. SUMMARY AND CONCLUSIONS

The screen printing technique is shown to be appropriate to prepare thick films of LSMO oxides. The technique is simple, can be easily scaled for large production, and using screened masks, films having the desired topology can be grown. Films of LSMO have been printed on polycrystalline Al$_2$O$_3$ substrates. However, the grain connectivity and film/substrate adherence are poor unless sintering temperatures around 1400 °C are used. Under these conditions, strong interdiffusion takes place between film which is not troublesome for the

magnetotransport properties of the films if they are made thick enough (above 10 μm). Of course, this difficulty can be solved if less reactive substrates could be used. A more interesting approach is the use of a melted additive to reduce the sintering temperature. We have shown that glass addition is moderately useful in this regard. Sintering glass/LSMO films at temperatures as low as 840 °C results in films of good mechanical properties if glass concentration of about 10% is used although with degraded LFMR.

According to the current understanding, electron scattering or tunneling at interfaces can be modified by magnetic decoupling of grains. Our work has established that using glass additives to make glass/LSMO composites, the LSMO grains are probably coated by the glass, but the low-field magnetoresistance does not increase. At most, it remains at the same level (20% at 5K) as without glass additives. The advantage of the lower sintering temperature still holds. However when the glass content rises above about 3%, the LFMR almost disappears, probably washed out by the more important nonmagnetoresistive contribution of the glass coating. Although solutions to overcome this problem are not presently evident, it appears that use of low melting temperature metallic materials, having smaller resistivities, may prove a convenient alternative.

ACKNOWLEDGMENTS

REFERENCES

1. S. Jin, T. H. Tiefel, M. McCormack, R. A. Fastnacht, R. Ramesh, and L. H. Chen, Science **264**, 2331 (1994).
2. H. Y. Hwang, S-W. Cheong, N. P. Ong, and B. Batlogg, Phys. Rev. Lett. **77**, 2041 (1996).
3. A. Gupta *et al.,* Phys. Rev. B **54**, R 15 629 (1996).
4. J. Fontcuberta, B. Martínez, V. Laukhin, Ll. Balcells, X. Obradors, C. H. Cohenca, and R. F. Jardim, Phil. Trans. R. Soc. London A **356** (1998).
5. N. D. Mathur, G. Burnell, S. P. Isaac, T. J. Jackson, B-S. Teo, J. L. MacManns-Driscoll, L. F. Cohen, J. E. Evetts, and M. G. Blamire, Nature (London) **387**, 266 (1997).
6. L. L. Balcells, R. Enrich, J. Fontcuberta, and X. Obradors, Appl. Phys. Lett. **69**, 1486 (1996).
7. *Ceramic Materials for Electronics,* edited by R. C. Buchanan (Marcel Dekker Inc., New York, 1991), Chap. 8.
8. *Thick Film Sensors,* edited by M. Prudenziati (Elsevier, New York, 1994), Sec. II.
9. G. Turilli and F. Licci, Phys. Rev. B **54**, 13 052 (1996).
10. A. Urushibara, Y. Moritomo, T. Arima, A. Asamitsu, G. Kido, and Y. Tokura, Phys. Rev. B **51**, 14 103 (1995).